PERFORMANCE AND FLOW CHARACTERIZATION OF A MARINE HYDROKINETIC TURBINE IN FREE SURFACE PROXIMITY

Nitin Kolekar, Ashwin Vinod and Arindam Banerjee[1]
Department of Mechanical Engineering & Mechanics,
Lehigh University, Bethlehem, PA 18015
[1]Corresponding author: arb612@lehigh.edu

INTRODUCTION

Marine hydrokinetic turbines (MHkT) operate in environments where the flow velocity and water depth undergoes cyclic variations that affect the performance characteristics of MHkT [1]. It is thus critical to understand effect of these variations on flow field and performance of MHkT. In addition, when the size of turbine is comparable to the channel size, flow acceleration takes place near the turbine rotation plane due to blockage offered by rotating turbine to the incoming flow [1, 2]. Blockage effects can be better understood by subdividing into a solid blockage and a wake blockage. The solid (bluff-body) blockage depends on area of turbine rotation disc relative to tidal channel (or river bed) cross section area. The wake blockage is primarily caused due to flow obstruction imposed by a counter-rotating wake that expands and dissipates behind the turbine. As the ratio of flow speed at blade tip to channel flow speed (defined as the tip speed ratio or *TSR*) is held constant at the design value, an increase in flow velocity increases the rotational speed; higher the turbine rotational speed, stronger the wake and higher the resultant wake blockage.

The effect of blockage on turbine performance has been studied previously [1, 3-7]. Chen and Liou [3] through their experimental investigations found that the blockage effect is strongly related to solid blockage, *TSR*, and blade pitch angle; higher blockage effects were observed at higher values of solid blockage and *TSR*. McTavish *et al.* [7] studied effect of blockage on initial wake expansion for different sized rotors in water channel using dye visualization technique. Higher blockage was found to narrow down the wake expansion and modify the vortex pairing behind the turbine. Furthermore, to take the advantage of higher flux near free surface, when a MHkT is installed in near-free surface environment it results in free surface deformation [1]. The proximity of turbine to the free surface provides additional restriction to flow behind turbine rotation plane. Several studies have also been performed to analyze effect of free surface proximity on turbine performance using porous discs to replicate the turbine rotors [4, 5, 8]. Myers & Bahaj [5] reported modifications in wake structure and recovery duration with varying disc to sea/bed and water surface proximity. Analytical and experimental study performed by Bahaj *et al.* [8] showed reduction in turbine power with decreasing blade tip-free surface clearance. Analytical models for performance prediction of turbine in free surface and blockage environment are based on application of linear momentum theory [9]. Flow visualization can be also used to account for blockage effects. Lartiga and Crawford [6] used flow field data from PIV measurements and CFD simulations to account for blockage effect in their actuator disc modeling. Manar *et al.* [10] performed an experimental study on a rotating wing in a confined space and concluded that the magnitude of measured blade forces was dependent on Reynolds number and blade-to-wall clearance. The measured lift coefficients were highest for the lowest tip clearance distance for which a stronger wall to tip vortex interaction was also observed resulting in dye entrainment off the wall into the tip vortex path. For a MHkT operating in near free surface environment similar phenomena are expected leading to modification of thrust and torque characteristics. However, flow entrainment in this case is expected to result in free surface deformation modifying the near-wake field and its propagation downstream the turbine which is one of the primary focus of current work.

Though there is an increasing interest in quantifying effects of blockage on performance and flow-field of turbine, majority of the reported experimental work for MHkT is limited to a turbine operating at single flow speed and/or single depth of immersion. The effect of free surface proximity on performance and flow dynamics of MHkT is not yet well understood. The principle goal of this article is to identify the governing mechanisms responsible for variation of turbine performance in free surface environment using carefully controlled laboratory experiments. We present the results of experimental campaign to study performance of MHkT operating in a near free surface environment. The blockage effects are quantified in terms of increase in flow velocity and power coefficient. Experimental data was adjusted according to blockage correction methodology adapted from Bahaj *et al*. [4] and Whelan *et al.* [9]. The experimental investigations are supported by stereo-PIV based flow-field visualization for the near-wake region for identification of flow structures associated with wake blockage and free surface deformation.

METHOD: FACILITY, EXPERIMENTAL SET-UP, AND FLOW VISUALIZATION

The experimental facility (see Figure 1) used for current study is an open surface recirculating water channel at Lehigh University with a test cross-section size of 0.61m×0.61m and length of 1.98m (Engineering Laboratory Design, USA). The turbine prototype used is a three bladed, constant chord, zero twist design with 0.14m radius. Additional details about the facility and model turbine can be found elsewhere [1]. Flow field investigations were carried out using a stereo-PIV system (TSI Inc.) to characterize wake structures, vortex structures, and flow in upper and lower bypass regions [11]. The flow medium was seeded with 13μm diameter hollow glass spheres (Potter Industries-SH400S20) that were illuminated with a 100mJ pulse, 100Hz, 532nm wavelength dual Nd:YAG laser. An in-situ calibration was performed with a dual plane target to determine the mapping functions between the image planes and actual measurement plane in the flow. A multi-pass frame-to-frame cross-correlation technique was employed to obtain 2D displacements in each image plane of the two cameras. A recursive Nyquist grid involving initial spot dimensions of 64 pixels×64 pixels and final spot dimensions of 32 pixels×32 pixels was employed for this purpose leading to 4.5×4.5 mm^2 interrogation region size. An effective overlap of 50% of the interrogation windows is employed in the PIV image processing. The 3D flow velocity vectors were then reconstructed by using the mapping functions obtained by the in-situ calibration procedure and the 2D displacements from each camera. A free-run PIV measurements were performed where a series of 2000 images were taken to determine the ensemble-averaged statistics of various flow quantities. Data from PIV flow visualization was then used to identify the flow structures in the near-wake region [$-0.5R \le X \le 1.4R$].

RESULTS AND DISCUSSION

To investigate the effect of free surface proximity and flow Reynolds number on turbine performance and near-wake flow structures, experiments were carried out with turbine operating at various flow velocities and immersion depths over a range of *TSR* values. The flow Reynolds number (Re_D) based on free stream velocity (specified tunnel velocity) and turbine diameter was varied from 8.2×10^4 to 2.2×10^5 which correspond to free stream flow velocity (U_∞) variation of 0.3m/s to 0.8m/s to quantify its influence on blockage effects. Experiments were performed with turbine rotating at various rotational speeds [30, 360] RPM to achieve a complete bell shaped C_p vs. *TSR* curve. Additionally, to understand the effect of free surface proximity on blockage effects, experimental runs were performed with turbine operating at various depths of immersions. The free surface proximity is expressed in terms of tip clearance ratio, $\delta h_U = h_U/D$, where, h_U represents water depth between turbine rotation disc and free surface and D represents turbine diameter. Table I presents details of experimental runs carried out during current study.

Table 1. FLOW VARIABLES AND TURBINE DEPTHS OF IMMERSIONS INVESTIGATED DURING CURRENT EXPERIMENTAL STUDY. [*Fr* is Froude number (ratio of characteristic flow velocity to the gravitational wave velocity= $U_\infty/\sqrt{gH}$) based on the channel depth]

U_∞ [m/s]	Re_D	Fr	δh_U
0.3	8.2×10^4	0.12	0.05, 0.27, 0.55
0.5	1.4×10^5	0.20	
0.7	1.9×10^5	0.29	
0.8	2.2×10^5	0.33	

Influence of Reynolds number on blockage effects

Figure 2 presents effect of Reynolds number on performance coefficient and flow acceleration (near turbine rotation plane) for δh_U of 0.55.

Measured values of C_p vs. TSR are plotted for flow velocities ranging from 0.3m/s to 0.8m/s (Figure 2a). An increase in flow velocity (hence Reynolds number) resulted in improved performance due to higher lift coefficients of SG6043 airfoil used for current turbine blades. The improvement in C_p started to diminish around Re_D of 1.9×10^5 (U_∞=0.7 m/s) beyond which C_p vs. TSR curve started to coincide irrespective of any increase in Reynolds number (except for the highest C_p point). Influence of blockage effects on percent change in U [$\%\Delta U = (U_F - U_\infty)/U_\infty \times 100$] for δh_U of 0.55 (U_F represents equivalent free stream velocity that will produce power similar to that of blocked case and is calculated based on blockage effects formulation) is presented in Figure 2b. These values represent flow acceleration near the turbine rotation plane due to blockage effects caused by presence of turbine compared to an undisturbed flow. Small values of $\%\Delta U$ for low TSR cases (TSR<3), indicate negligible blockage effects at low rotation speeds. As TSR increased beyond 3 (higher rotational speeds), blockage started altering the flow field yielding higher values compared to an unblocked case. This trend continued until maximum TSR case experimented during current study. The percentage change in U was found to be (almost) linearly increasing with TSR for lower Re, however, at higher Re and higher TSR, higher order variation was observed.

Effect of free surface proximity on blockage

To understand the effect of free surface proximity on turbine performance experiments were performed with different tip clearance ratios (δh_U=0.55, 0.27, and 0.05). Figure 3a compares measured experimental data for these three cases at channel flow velocity of 0.8m/s. Moving the turbine away from the channel bottom resulted in higher power coefficients due to higher wake blockage effects caused by deforming free surface behind the turbine. This trend continued until it reached an optimal tip clearance distance beyond which a reduction in performance was observed. Highest performance was attained for δh_U of 0.27 when turbine is submerged such that the turbine rotation disc is 0.076m ($\sim 0.5 \times R$) away from the free surface. In this case the free surface drop complemented the wake blockage that resulted in an improved turbine performance. When the turbine was moved further closer to the free surface (δh_U=0.05), performance degradation occurred due to penetration of wake by significant localized free surface drop observed behind turbine that adversely affected the turbine performance. These findings are further supported by results of flow visualization carried out in the near-wake of turbine and are discussed in next sub-section.

Figure 3b plots variation of percentage change in effective channel velocity as a function of δh_U for various TSR values. For all δh_U cases lower TSR values (<3) do not show any significant effect on flow acceleration near turbine plane. However, at higher TSR values (4.97, 6.62), a larger percent change was observed with respect to an unblocked case as well as between various δh_U cases. Larger percentage change at higher TSR values can be attributed to higher rotational speeds causing higher wake blockage effects. On the other hand, for a given TSR value, variation of $\%\Delta U$ with δh_U is due to the additional blockage caused by the free surface deformation. Higher the TSR, higher the free surface deformation and higher the blockage effect, as evidenced in Figure 3b. Depending on free surface proximity, the extent of this additional blockage differed in magnitude and inception. Maximum flow acceleration was found for the case with δh_U=0.27 for all TSR values.

Near-Wake Flow-Field in Presence of Blockage and Free Surface Proximity Effects

Flow visualization measurements based on stereo-PIV technique were carried out for U_∞=0.8m/s and RPM=180 at different depths of immersion to understand flow features in the wake and bypass regions that were responsible for improved performance in free surface-blocked environment. During present study, the PIV measurements were carried out with the laser sheet aligned to the stream wise direction (XY plane) and located at the blade root section ($z \cong 0.1 \times R$) as illustrated in Figure 1. For each rotational speed and tip clearance ratio, two sets of PIV measurements were carried out: first in the upper wake and second in the lower wake of the turbine. Images from these two measurements were stitched together to visualize complete near-wake flow and bypass flow up to $x \cong 1.5 \times R$.

Figure 4 plots contours of normalized stream-wise velocity ($U_{Normalized} = U/U_\infty$) for various tip clearance ratios. The horizontal dashed lines represent position of turbine tip and vertical solid lines correspond to turbine rotation plane. For the largest depth of immersion (δh_U=0.55), free surface is seen to have no effect on wake development behind turbine resulting in more or less symmetric structures around the turbine rotation axis. At the blade root position, a circular localized low velocity region (I) is observed, the size of which was of the order of blade root diameter. Wake starts to develop behind turbine rotation plane as a conical structure that expands downstream the turbine as depicted in Figure 4.

The regions near the turbine axis (wake-core) are observed to expand faster than the near tip (outer wake) regions. A localized high velocity region (IV) was developed right behind the blade root due to flow acceleration that occurs due to lower blockage near blade root that has smaller size compared to the blade chord (Figure 4a). Further, this region was followed by a region of comparatively lower velocity but still higher than rest of the wake. Thus, for the case of δh_U = 0.55, no significant difference was observed between the flow structures in the upper bypass and lower bypass regions, alluding absence of free surface blockage effects.

On the other hand, Figure 4b presents contours of stream-wise velocity for the case of δh_U = 0.27. It was observed that clearance ratios 0.55 and 0.27 lead to similar shape of lower wake region (III) but significantly different upper wake regions (II). For δh_U = 0.27, the wake expansion in radial direction for upper wake is limited by faster moving upper bypass region (compare Region II in Figure 4a and 4b). Free surface deformation behind the turbine rotation plane led to flow structure modifications, particularly in upper bypass and upper wake regions resulting in wake compression and faster upper bypass flow that was responsible for improved turbine performance.

For δh_U=0.05 (Figures 4c), lower wake region exhibited flow structures similar to δh_U=0.27 case, however upper wake was significantly different due to localized free surface drop that penetrated not only into the upper bypass but also into the upper wake region. The tip vortex structures bounding the wake region were washed away by the free surface drop without any significant modifications of the lower wake and tip vortices below the turbine axis. The localized free surface deformation in this case is associated with downward flow velocity that creates localized high pressure zone behind the turbine (in the near-upper-wake region). This reduces effective Δp across the turbine decreasing its power output.

Thus for MHkT operating in a free surface environment, the wake is highly asymmetric due to free surface deformation behind the turbine rotation plane, the extent of which depended on δh_U values. Free surface deformation and associated bypass acceleration and wake compression resulted in performance improvement for δh_U = 0.27 while localized free surface drop for δh_U = 0.05 resulted in wake penetration adversely affecting the performance.

CONCLUSIONS

The results of experimental investigations to quantify the effect of free surface proximity and associated blockage effects on performance and flow-field of MHkT are presented. Experiments were carried out with turbine operating at various flow velocities [U = 0.3m/s-0.8m/s] and tip clearance ratios [δh_U= 0.05, 0.27, 0.55] over a range of *TSR* values [1-8]. Higher flow velocities and higher rotational speeds were found to increase the blockage effects improving the torque and thrust loading compared to the unblocked case. Improvement in performance was attributed to accelerated bypass flow velocity (upto 14% increase) that was quantified with a blockage correction formulation. Additionally, experimental study to investigate the effect of free surface proximity on blockage effects revealed deformation of the free surface behind turbine rotational plane leading to asymmetric wake for a turbine operating at high free surface proximity. The shape and intensity of free surface drop was found to be dependent on flow velocity, rotational speed and tip clearance distance. Maximum improvement in turbine performance characteristics (compared to unblocked cases) was observed for δh_U= 0.27. In this case, the additional bypass flow acceleration and wake compression provided by the free surface deformation complimented the total blockage. Moving the turbine further closer to the free surface (δh_U= 0.05) caused localized free surface drop that penetrated into the upper wake. This resulted in reduced Δp across the turbine adversely affecting its performance.

REFERENCES

1. Kolekar, N. and A. Banerjee, *Performance characterization and placement of a marine hydrokinetic turbine in a tidal channel under boundary proximity and free surface effects.* Journal of Applied Energy, 2015. **148**: p. 121-133.
2. Maskell, E.C.A.R.C.L., *A Theory of the Blockage Effects on Bluff Bodies and Stalled Wings in a Closed Wind Tunnel*. 1963, Ft. Belvoir: Defense Technical Information Center.
3. Chen, T.Y. and L.R. Liou, *Blockage corrections in wind tunnel tests of small horizontal-axis wind turbines.* Experimental Thermal and Fluid Science, 2011. **35**(3): p. 565-569.
4. Bahaj, A.S., et al., *Power and thrust measurements of marine current turbines under various hydrodynamic flow conditions in a cavitation tunnel and a towing tank.* Renewable Energy, 2007. **32**(3): p. 407-426.
5. Myers, L.E. and A.S. Bahaj. *The effect of boundary proximity upon the wake structure of horizontal axis marine current turbines*. in *27th International Conference on Offshore Mechanics and Arctic Engineering (OMAE 2008)*. 2008: The American Society of Mechanical Engineers.
6. Lartiga, C. and C. Crawford, *Actuator disk modelling in support of tidal turbine rotor testing*, in *3rd Int. Conf. on Ocean Energy*. 2010: Bilbao, Spain, .

7. McTavish, S., D. Feszty, and F. Nitzsche, *An experimental and computational assessment of blockage effects on wind turbine wake development.* Wind Energy, 2013.

8. Bahaj, A.S., et al., *The Effect of Boundary Proximity Upon the Wake Structure of Horizontal Axis Marine Current Turbines.* Journal of Offshore Mechanics and Arctic Engineering, 2011. **134**(2).

9. Whelan, J.I., J.M.R. Graham, and J. Peiro, *A free-surface and blockage correction for tidal turbines.* J. Fluid Mech., 2009. **624**: p. 281 - 291.

10. Manar, F., A. Medina, and A. Jones, *Tip vortex structure and aerodynamic loading on rotating wings in confined spaces.* Experiments in Fluids, 2014. **55**(9): p. 1-18.

11. Adrian, R.J., *Particle-Imaging Techniques for Experimental Fluid Mechanics.* Annual Review of Fluid Mechanics, 1991. **23**(1): p. 261-304.

FIGURES

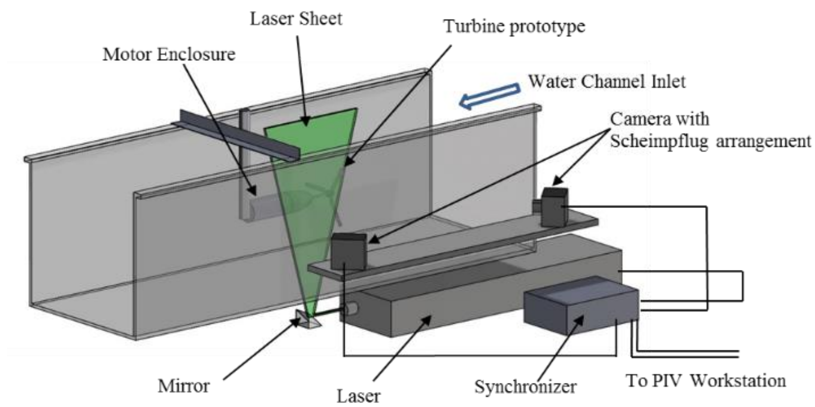

Fig. 1. Experimental set up for flow field measurements with stereoscopic PIV

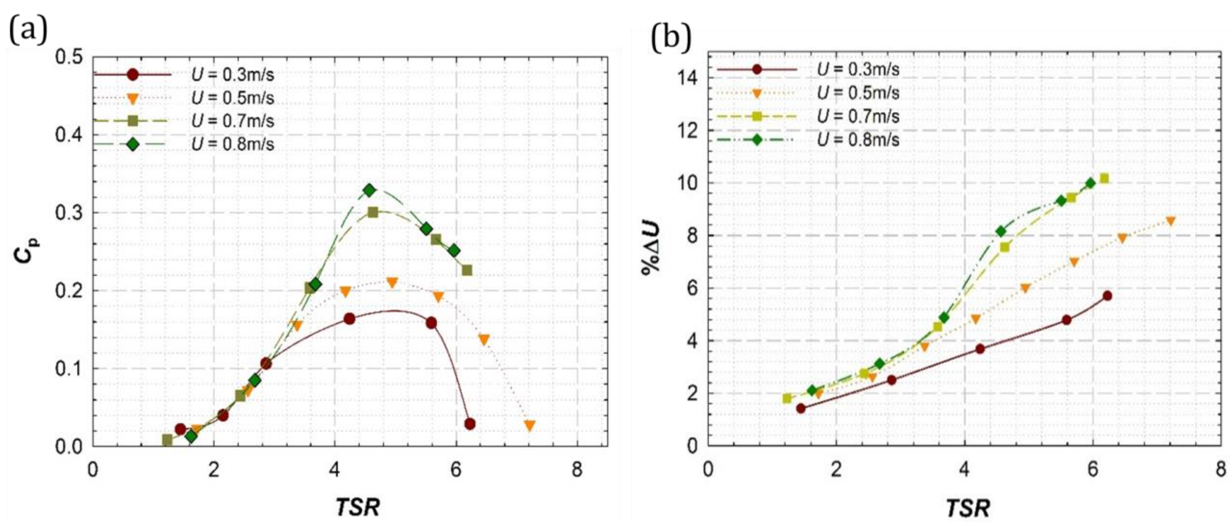

Fig. 2: Effect of Reynolds number on (a) measured power coefficient and (b) calculated flow acceleration for δh_U = 0.55

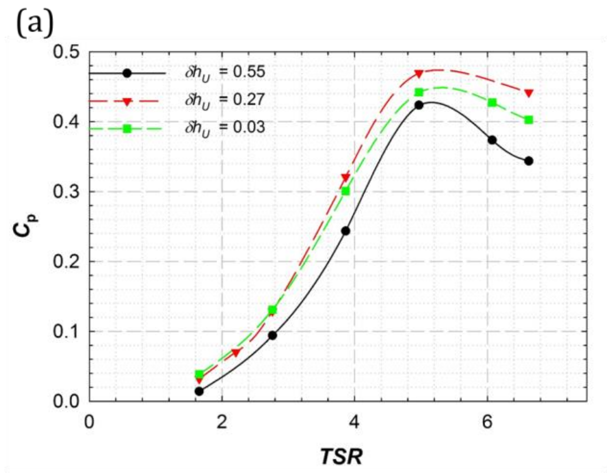

Fig. 3: Variation of (a) measured C_p and (b) calculated flow acceleration with depth of immersion for U=0.8m/s

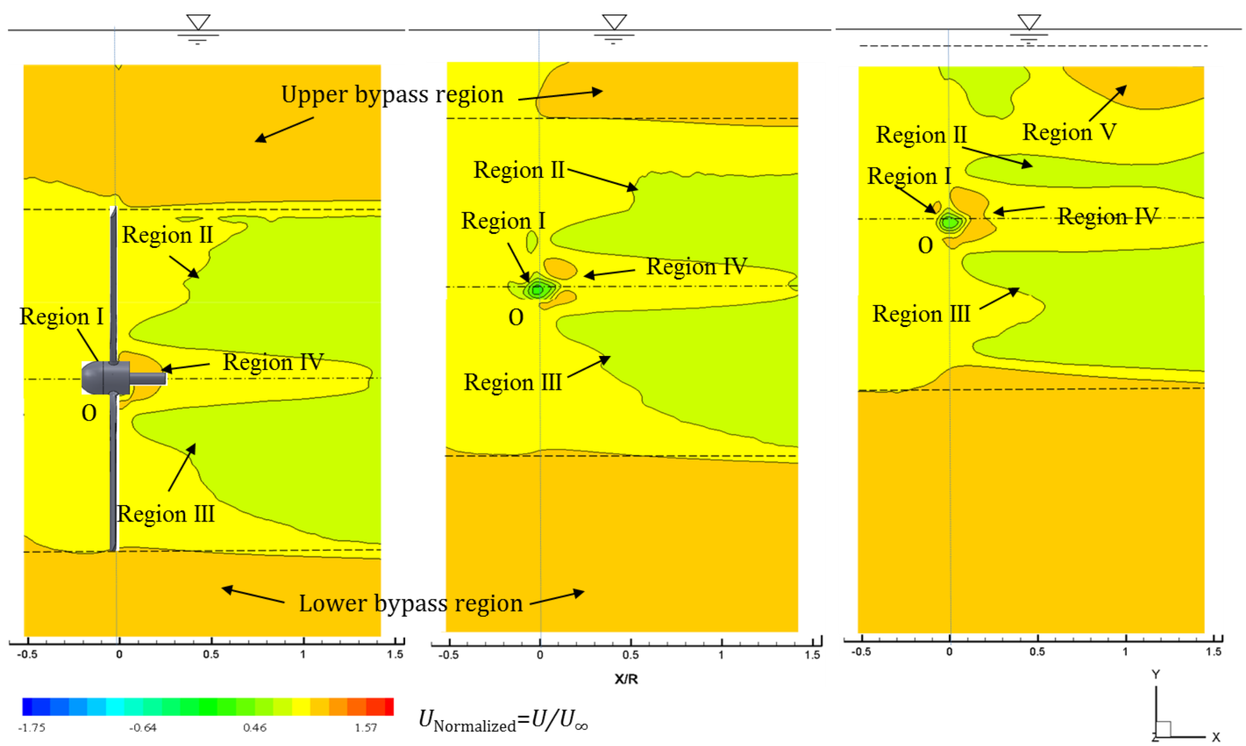

(a) (b) (c)

Fig. 4: Time averaged contours of stream-wise velocity at rotational speed of 180RPM for tip clearance ratio of (a) δh_U = 0.55, (b) δh_U = 0.27, and (c) δh_U = 0.05 (horizontal axis represents normalized stream-wise distance form turbine rotation plane=X/R